



Intra-day co-movements of crude oil futures: China and the international benchmarks

Qiang Ji¹ · Dayong Zhang² · Yuqian Zhao³

Accepted: 28 April 2021 / Published online: 15 May 2021

© The Author(s), under exclusive licence to Springer Science+Business Media, LLC, part of Springer Nature 2021

Abstract

Investigating the co-movements between crude oil futures helps to understand the integration of the global markets. This paper focuses on Shanghai crude oil futures (INE) and study its co-movements with the international benchmarks of WTI and Brent crude oil futures in intra-day day and night trading sessions. A complex network model framework is proposed to analyse the intra-day co-movement patterns labelled by a functional data clustering approach on intra-day return curves. Our findings indicate INE is more integrated with the global market during the night session, but it shows a regional fractional effect during the day session. Based on the revealed dynamics of co-movement patterns, we further design a pairs trading strategy between INE crude oil futures and the international benchmarks. The simulation results show that the pairs trading strategy can be promisingly profitable, even during market turmoil phases.

Keywords INE Crude oil futures · WTI and Brent · Intra-day co-movement patterns · Complex network model · Pairs trading

JEL Classification C12 · C52 · G11 · G15

1 Introduction

Since the financial crisis of 2008, the pricing pattern in the international crude oil market has become more complex and sometimes impenetrable. A more volatile and less predictable

✉ Qiang Ji
jqwxnjq@casipm.ac.cn

Dayong Zhang
zhangdayong@gmail.com ; dzhang@swufe.edu.cn

Yuqian Zhao
y.zhao@essex.ac.uk

¹ Institutes of Science and Development, Chinese Academy of Sciences, Beijing, China

² Research Institute of Economics and Management, Southwestern University of Finance and Economics, Chengdu, China

³ Essex Business School, University of Essex, Colchester, UK

market is partly due to the aftermath of the crisis and partly due to the dramatic changes in the global markets. For example, the shale gas revolution brought the U.S. energy independence, which has greatly changed the global oil trade network. Since 2014, the price war led by Saudi Arabia and OPEC drove oil prices to a level lower than the crisis period. Pressures from climate change have made the energy transition more urgent. As more countries committed carbon-neutral, replacing traditional fossil fuel energy with renewables will be faster. The transition process will inevitably press international crude oil markets further. In addition, geopolitical risks cannot be ignored when we investigate the global crude oil markets. Brexit, the US-China trade war, the anti-globalization, and the COVID-19 pandemic are disturbing forces that shake the foundation of the current crude oil system and bring new changes to the global energy landscape.

An important topic in studying crude oil futures markets is whether worldwide comprise an integrated global market or regional fractional markets. The impetus behind this is that markets-based rules have gradually driven the asset pricing of crude oil futures. Studying the co-movements and the lead-lag effect between different markets also provides a theoretical basis for global investors who participate in spread trading and risk hedging in crude oil futures markets. In the global crude oil trading system, China nowadays plays an increasingly important role since it has become the world's largest crude oil importer. It is non-negligible to consider the effect of crude oil prices in China on the global crude oil pricing system, given the fact that the demand of emerging markets is a significant factor since 2003 (Li and Lin 2011). As a result, this motivates studies of co-movements between China's market and the international crude oil markets.

Prior to 2018, most studies in this field concentrated on analyzing the co-movement or spillover effect between the Chinese spot market and the international crude oil futures markets. In general, significant co-movement characteristics were empirically evidenced. Li and Leung (2011) found that China was actively engaged in the world oil market and formed a cointegrated relationship with major international crude oil futures. Jia et al. (2015) applied multivariate dynamic correlation models to test the dynamic co-movement between Chinese Daqing spot prices and three crude oil futures, including Brent, Dubai, and Minas. Their results suggested a global integration of crude oil markets. Zhang (2019) also investigated the integration between Chinese Daqing crude oil spot and WTI crude oil futures and found a significant spillover effect in returns and volatilities.

On March 26, 2018, crude oil futures were officially listed on the Shanghai International Energy Exchange (INE), which instantly received extensive attention from global traders (Ji and Zhang 2019). This market then experienced rapid development during the following three years, such that Shanghai crude oil futures exceeded Oman crude oil futures in terms of the trading volume. Today, they are the most frequently traded crude oil futures in Asia and has become the world's third-largest crude oil futures trading product after WTI and Brent. In 2020, this growing trend did not be halted in the presence of the outbreak of the COVID-19 pandemic. Instead, because of the demand for safe-haven hedging from other sectors, the volume of INE crude oil futures has achieved extensive growth during the pandemic. In June 2020, the average daily trading volume reached 300,000 transactions, and the average daily open interest exceeded 150,000, carrying out a threefold and fourfold increase from the beginning of the year, respectively. Besides, INE crude oil futures were initially more actively traded during night trading sessions because more information was revealed in Western trading hours. In contrast, the current trading volume during daily trading sessions has increased in proportion from 25% in 2018 to 50% in 2020. On some trading days, the liquidity during Asian main trading hours has exceeded that of Brent crude oil futures, indicating that INE is progressively dominating investors in Asian trading hours.

The integration between WTI and Brent has been extensively studied. Overall, these two futures show strong co-movements, although the discussions about their dynamic relationships are still controversial. On the one hand, some evidence of a long-run relationship among these two crude oil futures was identified, see, Hammoudeh et al. (2008), AlMadi and Zhang (2011), and Narayan et al. (2011). Also, Klein (2018) verified that OPEC meetings could increase the correlation between WTI and Brent in the short run, while WTI shows price leadership over Brent in spot and futures. On the other hand, some recent studies claimed that the US shale oil supply shock had broken the long-run relationship between WTI and Brent. Ji and Fan (2015) found a new structural break in the relationship between regional crude oil prices, which could be attributed to the decoupling of WTI from other crude oils since 2010. In addition, the authors concluded that WTI was a price setter before 2010, while Brent has become a leading role since 2011. Chen et al. (2015) identified the same breakpoint and stated that WTI had appeared to trade at a sizeable discount against Brent in recent years. Such a spread implies arbitrage and hedging opportunities, also see Caporin et al. (2019).

More recently, as a new market participant, INE crude oil futures receive trendy attention to study its co-movements and regional fractional effect with the global benchmark crude oil futures. The existed works mainly focused on the pricing rule and market efficiency of INE as a single market (Ji and Zhang 2019; Li et al. 2020; Yang et al. 2019; Wang et al. 2019). Only a few works have been done to study the dynamic co-movements between INE and international crude oil futures to the best of our knowledge. Palao et al. (2020) applied a multiple regression model to examine the impact of INE on WTI and Brent. The findings showed that INE exhibited limited influence on the intentional market. In a more related study, Huang and Huang (2020) asserted weak and unstable co-movements between WTI, Brent, and China's crude oil futures by using daily closing prices. Their results revealed market co-movement patterns in both short-run and long-run, providing implications to regulators and investors.

However, the informative high-frequency data so far has not been studied. The intra-day information is particularly of interest in this study because it contains additional trading information and allows us to investigate the co-movements between crude oil futures in day and night trading sessions separately. Segmenting intra-day trading hours into day and night trading sessions is a regulatory rule of INE crude oil futures. As a consequence, it is likely to have differently behaved investors in these two trading sessions (Ji and Zhang 2019). Hence, dissecting the intra-day co-movements between INE and the representative international crude oil futures is a question worthy of study.

In this paper, we consider intra-day return curves of INE, WTI, and Brent crude oil futures. The data is collected at a five-minute frequency from March 26, 2018, to April 30, 2020. By smoothing the discrete data into intra-day return curves, we classify the intra-day movement patterns into three categories, "Rise", "Decrease", and "Sidewalk" through a functional data clustering approach. The labelled intra-day co-movement patterns allow us to set up complex network models to depict the dynamic interrelationships among these three crude oil futures. According to the empirical results, INE shows more integrated co-movements with WTI and Brent crude oil futures during the night trading session; INE behaves more like a regional fractional market to the intentional markets during the day trading session. The results indicate that investors in China's crude oil futures market are more inclined to be affected by global macroscopic news during WTI and Brent's active trading hours. Besides, by splitting the sample into sub-samples of a market normal phase and a COVID-19 pandemic phase, we notice that INE shows fewer co-movements with the international under the local market regulations during the market turmoil, providing implications to investors for hedging risks.

To study the dynamic intra-day co-movement patterns, this paper applies complex network models embedded with a functional data analysis to tackle the high-frequency information. Conventionally, realised and range-based measurements are usually used to study data in a high-frequency environment. Such econometric methods calibrate the objective variance or covariance estimators by incorporating intra-day information, but intra-day movement patterns can be omitted. Instead, we smooth the discrete high-frequency data into functional intra-day curves. This is a more rational treatment because (1) functional intra-day curves effectively preserve the intra-day movement patterns; (2) intra-day price or return data observed on a very fine grid are intrinsically forming a continuous functional curve. We refer to the recent papers by Kearney and Shang (2020) and Rice et al. (2020a) on functional data analysis applications in finance.

The contributions of this paper can be summarized three-fold. First, our results complement the findings of Huang and Huang (2020), who claimed that INE shows fewer co-movements with WTI and Brent. We recognize that market regulations lead to a relatively segmented day-night market for INE crude oil futures, and our empirical results show that co-movements between INE and the other two benchmarks can be strong during the night trading sessions. In addition, the distinctive regional difference during the day trading session generates hedging opportunities for domestic and international investors. Second, based on intra-day co-movements dynamics, we implement a pairs trading strategy between INE and international benchmarks. The simulation results indicate a profitable trading strategy, even during the market crisis. This is useful for investors and also provide further implications to regulators in studying the regional effect. Third, we propose a methodological framework to investigate the dynamics of intra-day co-movements in financial markets. The framework can be applied to study co-movements in other financial markets and potentially useful for setting up more complicated trading strategies.

The remainder of the paper is structured as follows. Section 2 describes the dataset and the main methodology, including a functional data clustering approach and a complex network model method. Section 3 summarises the empirical results. In Sect. 4, based on the intra-day co-movement patterns, we design a pairs trading strategy between WTI, Brent, and INE, and their performances are assessed under both market normal and the COVID-19 pandemic phases. Section 5 concludes and provides policy implications.

2 Data and methodology

This section first introduces the intra-day crude oil futures dataset and then outlines a complex network analysis framework to study the intra-day co-movement patterns between China's and international crude oil futures.

2.1 Intra-day crude oil futures dataset

The dataset used in this study is composed of INE, WTI, and Brent crude oil futures intra-day price data at a five-minute frequency, collected from WIND and Thomson Reuters Eikon databases. The time series price data is formed by using the front-month futures contracts for all three assets. The sample starts when INE first listed its contracts until the recent outbreak (i.e., the first surge phase) of the COVID-19 pandemic, ranging between March 26, 2018, and April 30, 2020.

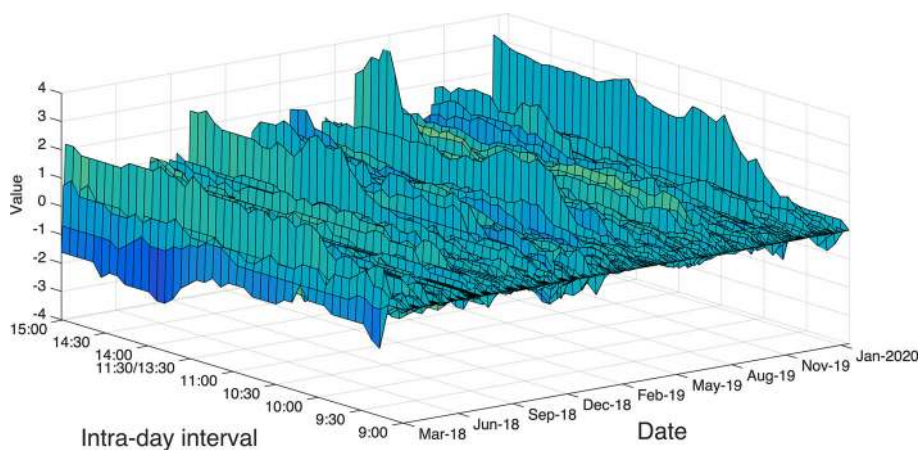


Fig. 1 CIDR curves for INE over the day trading session

Because INE crude oil futures are traded under specific regulatory rules, we tailor our sample for the main context analysis from the following two aspects. First, INE crude oil futures only trade on weekdays in separate day trading sessions (9:00 a.m.–11:30 a.m. and 1:30 p.m.–3:00 p.m.) and night trading sessions (9:00 p.m.–2:30 a.m.). To ensure that the consistent information flow is used, we consider two continuous trading sessions: day (9:00 a.m.–3:00 p.m.) and night (9:00 p.m.–2:30 a.m.) for all three crude oil futures according to their local trading times. Second, due to the concern of the catastrophic effect of the COVID-19 pandemic, INE suppressed its night trading session from January 22 to May 6, 2020. Therefore, we truncate our sample until January 22, 2020, for a market normal phase analysis. The trading information between January 22 and April 30, 2020, is used for robustness check analysis over the COVID-19 pandemic in Sect. 4.2.

In both sub-samples, we obtain two intra-day price curves from day and night trading sessions on each trading day by smoothing high-frequency discrete price data into functional curves through B-spline functions (Ramsay and Silverman 2007). We denote the price curve as $P_i(t)$, for $1 \leq i \leq N$ and $t \in [0, 1]$, where N is the sample size and t is the intra-day standardised index. As functional data objects, the price curves are assumed to be random sequences in $L^2[0, 1]$ Hilbert space with sample-path on $[0, 1]$. For a stationary transformation, we use the cumulative intra-day log return curves (CIDR) $y_i(t)$ as discussed in Kokoszka et al. (2017), formulated as,

$$y_i(t) = 100 \times (\log P_i(t) - \log P_i(0)), \quad 1 \leq i \leq N, \quad t \in [0, 1], \quad (1)$$

where $P_i(0)$ is the opening price on day i . There are other versions of intra-day return curves; see, Kokoszka et al. (2017) and Rice et al. (2020b). We choose the CIDR curve because its smoothness naturally serves to a functional data analysis modelling. More importantly, the CIDR curves can be classified based on the well-preserved intra-day movements, enhancing our understanding of the evolutions of intra-day returns for crude oil futures. In a visual example, Fig. 1 displays the trajectory of INE's CIDR curves over the day trading sessions from March 2018 to January 2020.

Table 1 provides a statistical summary of the returns, where Panel A documents the properties of discrete intra-day returns. The results indicate an inverse day-night effect between INE and the international benchmarks. INE gains negative averaged returns and large fluctu-

tuations during the night trading session, while WTI and Brent obtain positive and smaller counterparts, respectively. Panel B shows the properties of the CIDR curves by applying recently developed hypothesis tests in functional time series analysis, including the stationary test (\mathcal{H}_0 : stationary curve, Horváth et al. 2014), the normality test (\mathcal{H}_0 : Gaussian-typed curve, Górecki et al. 2018), the autocorrelation test (\mathcal{H}_0 : uncorrelated but a heteroscedastic curve, Kokoszka et al. 2017) and the conditional heteroscedasticity test (\mathcal{H}_0 : independent curve, Rice et al. 2020b). The autocorrelation and heteroscedasticity are examined with maximal lag H up to 20. We find that the CIDR curves drawn from crude oil future markets, like other typical financial asset returns, are stationary, non-normal, uncorrelated, and conditional heteroscedastic.

2.2 Methodology

We now introduce a complex network analysis framework embedded with a functional data clustering approach. Complex network analysis has been successfully applied to many fields, including economics and finance. This method provides a topological structure to depict the dynamic relationship between objects, which tallies with the interests of many financial research topics. For example, Gai and Kapadia (2010) designed a financial network model to study the contagion effect in the equity market. Zhu et al. (2018) segmented the co-movement patterns of equity indexes into positive, none, and negative categories and built a complex network model to investigate financial contagions (also see Wang et al. 2016). The popularity of the complex network model protrudes its flexibility as the objects can be numeric variables or symbolic characters. Thus, in order to investigate the intra-day dynamics of crude oil returns, we first classify the intra-day return curves into categories according to their movement patterns and then build complex network models to explore the interrelationships.

The intra-day movement classification is completed by using a functional data clustering approach proposed in Bouveyron et al. (2015). One can refer to Sugar and James (2003) and Bouveyron and Jacques (2011) for other relevant methods. We apply a functional mixture model-based approach—the FunFEM algorithm (Bouveyron et al. 2015), because it is more effective to fit spike-like financial data and allows for the visualisation of the clustered groups. To describe this approach, we consider a set of known basis functions $\{\psi_1(t), \dots, \psi_p(t)\}$, $t \in [0, 1]$. In functional data analysis, the CIDR curves $y_i(t)$ can be approximated as:

$$y_i(t) = \sum_{j=1}^p \gamma_j \psi_j(t),$$

where the loading coefficient $\Gamma = \{\gamma_1, \dots, \gamma_p\}$ is a random vector on \mathbb{R}^p . Our goal is to classify $y_i(t)$ into M homogeneous groups using a discriminate functional model. For the model construction, we assume the latent random variable $g_m \in \{g_1, \dots, g_M\}$ to aid the group identification of $y(t)$. Under the rules, the model obtains $g_m = 1$ if $y(t)$ belongs to the m th group; otherwise, it is valued 0. Hence, based on the estimator of $g_{i,m}$, we identify the group index for each CIDR curve $y_i(t)$. We also assume that the most discriminative subspace in the M groups is spanned over d known basis functions $\{\phi_1, \dots, \phi_d\}$, for $d < M$ and $d < p$. Projecting $y_i(t)$ onto $\{\phi_j\}$, $j \in [1, d]$ bases, we get the random functional loadings $\Lambda = \{\lambda_1, \dots, \lambda_d\} \in \mathbb{R}^d$. The following linear transformation then connects the basis functions ψ_j , $1 \leq j \leq p$ and ϕ_j , $1 \leq j \leq m$,

$$\Gamma = U\Lambda + \varepsilon,$$

Table 1 Statistical summary of crude oil intra-day returns with the P-values of the autocorrelation, conditional heteroscedasticity, normality and stationary hypotheses testing

	Average	SD	Skewness	Kurtosis	Min	Max	Median		
<i>Panel A: discrete intra-day returns</i>									
INE _{day}	0.0069	0.5254	− 0.0695	6.0269	− 3.0772	4.3761	0.00		
INE _{night}	− 0.0371	0.9615	− 0.2183	5.2088	− 5.8875	6.8259	0.00		
WTI _{day}	− 0.0557	1.1089	− 0.1659	4.0822	− 7.3526	7.3793	− 0.0141		
WTI _{night}	0.0049	0.3824	0.0896	13.2216	− 3.9360	3.6210	0.00		
Brent _{day}	− 0.0564	0.9157	− 0.2321	5.6462	− 6.7600	6.1120	0.00		
Brent _{night}	0.0066	0.4026	0.0495	11.2758	− 3.1418	3.6077	0.00		
<i>Panel B: CIDR curves</i>									
	Autocorrelation			Heteroscedasticity			Normality	Stationarity	
Lag	<i>H</i> = 1	<i>H</i> = 5	<i>H</i> = 10	<i>H</i> = 20	<i>H</i> = 1	<i>H</i> = 5	<i>H</i> = 10	<i>H</i> = 20	
INE _{day}	0.48	0.46	0.42	0.50	0.44	0.00	0.00	0.00	0.79
INE _{night}	0.67	0.27	0.31	0.38	0.51	0.00	0.01	0.12	0.82
WTI _{day}	0.21	0.30	0.59	0.75	0.43	0.00	0.02	0.00	0.83
WTI _{night}	0.57	0.76	0.87	0.91	0.58	0.00	0.00	0.28	0.55
Brent _{day}	0.76	0.35	0.50	0.59	0.09	0.00	0.00	0.00	0.87
Brent _{night}	0.61	0.39	0.47	0.52	0.45	0.00	0.00	0.16	0.40

where U is a $p \times d$ coefficient matrix, and $\varepsilon \in \mathbb{R}^p$ is an independent noise term. We further assume that conditional on g_m , Λ is multivariate Gaussian distributed: $\Lambda|g_m \sim \mathcal{N}(\mu_m, \Sigma_m)$, where μ_m and Σ_m are the mean and the covariance matrix of the m th group, respectively. In terms of the noise term, a multivariate Gaussian density $\varepsilon \sim \mathcal{N}(0, \Xi)$ is assumed such that the covariance matrix $\Pi_m = \text{cov}([U, V]^\top \Gamma | g_m) = [U, V]^\top \Sigma_m [U, V]$ is expressed as follows:

$$\Pi_m = \begin{bmatrix} \Sigma_m & 0 \\ \beta & 0 \\ 0 & \ddots \\ 0 & 0 & \beta \end{bmatrix},$$

where Σ_m represents the variance of $y_i(t)$ categorized into the m th group, and β is the variance of the noise term.

As indicated by Bouveyron et al. (2015), twelve discriminative functional models can be formed through different constraints on Π_m . A FunFEM algorithm with three steps then solves these discriminative functional models: (1) assuming posterior probabilities to unknown group functions; (2) applying the EM algorithm to solve the model given a known group functions assumed in step (1); (3) updating the posterior probabilities and iterating steps (1) and (2) until a criterion is reached. The optimal discriminative model is then selected through the penalised criteria discussed in Birgé and Massart (2007) and then provides advice on the data clustering. For more technical details about the FunFEM algorithm, we refer to Bouveyron et al. (2015).

The crude oil futures CIDR curves thus can be clustered into three movement patterns – “Rise” (r), “Sidewalk” (d), and “Decrease” (d) via the above method. We now construct complex network models on the clustered intra-day return curves. The networks are used to study the intra-day dynamics of a single asset or the co-movement between multiple assets. We, therefore, define the intra-day mode of crude oil futures in two forms: (1) {Day-pattern, Night-pattern}, (2) {INE pattern, benchmark pattern}. The former depicts a single asset’s intra-day return movement pattern. For example, suppose the day and night trading sessions were “Rise” and “Sidewalk” for INE on the day (i), we label a pattern “rs” on the day (i). The latter describes the co-movement dynamics between INE and the benchmark crude oil futures. In this form, the “rs” represents that the CIDR curves are categorized as “Rise” and “Sidewalk” for INE and benchmark crude oil futures on the day (i), respectively.

Following Gai and Kapadia (2010), we consider a network structure with $K = 9$ nodes, which are the permutations of two elements between three patterns: “r”, “s” and “d”. The network nodes represent different intra-day modes, and the edges between nodes indicate the direction and weight of the indicated transformation. To understand the properties of the networks, we concentrate on three measures that capture key features of the structure: degree, betweenness, and closeness centralities. The degree centrality depicts how many connections one node has, consisting of an in-degree and out-degree in a directional network, representing incoming and outgoing connections to a node. In the formula, for node u , $u \in [1, 9]$, the degree D_u measures the total number of connections $c_{u,v}$ by:

$$D_u = \sum_v^{J_{u,in}} c_{u,v} + \sum_v^{J_{u,out}} c_{u,v},$$

where $J_{u,in}$ and $J_{u,out}$ are the number of neighbours of node u in terms of incoming and outgoing directions, respectively. The degree indicates which nodes are the most frequent in the network structure.

Betweenness centrality identifies the transition ability of node u , measuring the number of the shortest paths from all nodes to others that pass through the node u . To formulate it, we denote the betweenness of node u by B_u as follows:

$$B_u = \sum_v^{\mathcal{K}} \sum_k^{\mathcal{K}} \frac{g_{v,k}(u)}{g_{v,k}},$$

where $g_{v,k}(u)$ is the number of the shortest paths that pass through node u . Therefore, the node with a higher betweenness plays a more important mediating role in the network.

The third measurement is closeness centrality, which is defined as the distance from a node to all other nodes in the network. Specifically, in node u , its closeness C_u is the sum of the shortest distances between node u and all others, given as follows,

$$C_u = \sum_{v=1}^{\mathcal{K}_u} d_{u,v}, \quad \mathcal{K}_u \leq \mathcal{K},$$

where $d_{u,v}$ is the shortest distance between node u and v , and \mathcal{K}_u is the total number of nodes that connects with node u .

3 Empirical results of complex network models

3.1 The clustering of CIDR curves

This section conducts complex network analyses and studies the intra-day dynamic (co-)movements of crude oil futures. Based on the FunFEM algorithm, the CIDR curves are clustered into “r”, “s” and “d” modes, revealing their intra-day movement patterns. Figure 2 displays the clustered CIDR curves of INE, WTI, and Brent crude oil futures in both day and night trading sessions. In accordance with the findings shown in Table 1, we find a day-night reversal effect. INE’s returns from the day trading sessions lack trading activity and exhibit less variation, which is similar to the behaviour of WTI and Brent from the night trading sessions. Conversely, INE’s returns become more fluctuated during the night trading session, roughly mimicking WTI and Brent’s movement patterns during their day trading sessions. This result meets our expectation because WTI and Brent crude oil futures are more active during their day trading sessions, and investors from the Shanghai futures exchange during the night trading session mainly follow the information conveyed from the international benchmarks. We explain this result with the characteristic that China’s crude oil futures market lacks international investors, given the market access barriers discussed in Huang and Huang (2020).

Besides, we compute the proportions of three modes for each of crude oil futures. Figure 3 illustrates the portions of “Rise”, “Sidewalk” and “Decrease” intra-day movement patterns over the day and night trading sessions in the entire sample for INE, WTI, and Brent crude oil futures. From the figure, we observe that for all three assets, around one-half of the CIDR curves fall into a pattern of “Sidewalk” intra-day movement, and the “Rise” and “Decrease” intra-day movement patterns roughly share the remaining portions equally. Comparatively, WTI and Brent behave similarly in all three intra-day movement patterns in both day and night trading sessions. INE is more likely to present a “Sidewalk” pattern in the day trading sessions, but it is inclined to show directional patterns in the night trading sessions. This

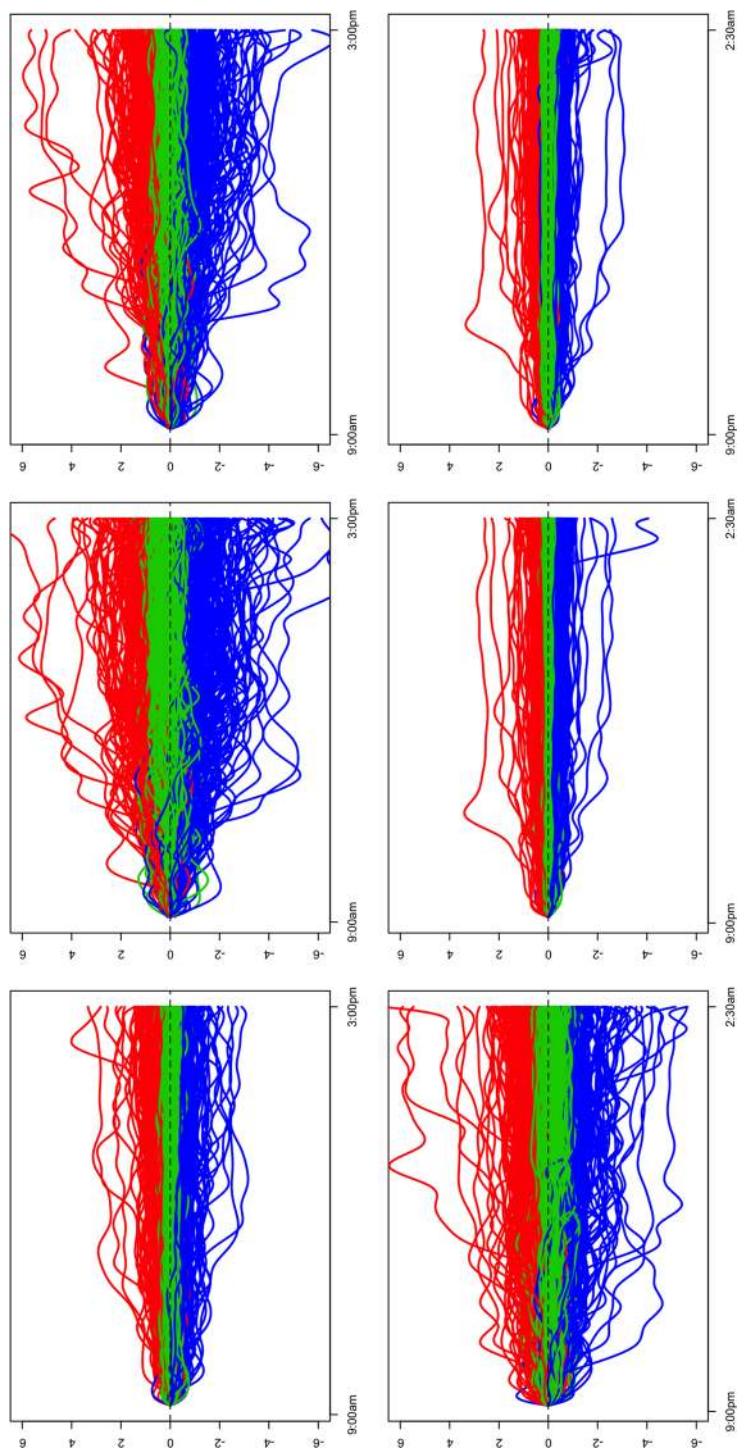


Fig. 2 Clustering of CIDR curves on INE, WTI and Brent crude oils over the day and night trading sessions. The sub-figures in the first, second and third columns represent INE, WTI and Brent, and the sub-figures in the first and second rows represent day and night trading sessions

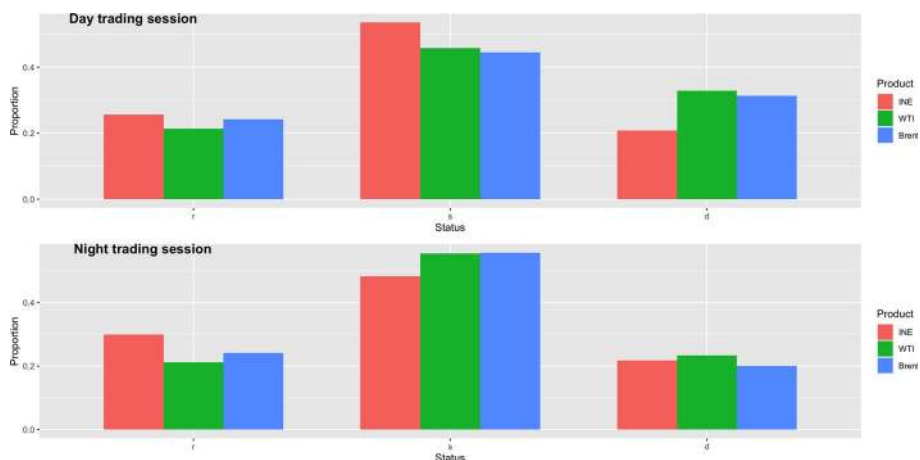


Fig. 3 Proportions of intra-day movement status on INE, WTI and Brent crude oils. The sub-figures in the first and second rows represent day and night trading sessions

result confirms that INE retains market follower's role to the WTI and Brent crude oil futures during the night trading sessions.

3.2 Complex networks analysis

We then investigate the interrelationships between the nodes labelled by clustered intra-day modes with the complex network analysis. Let us first focus on the single asset crude oil futures. The network nodes are formed as intra-day movement modes {Day-pattern, Night-pattern}. Figure 4 displays three complex networks built for INE, WTI, and Brent crude oil futures, respectively. In the network models, the nodes with larger scales imply higher degrees, and a thicker directional edge indicates more weight on such transformations, that is, a more frequent transformation from one node to another.

By combining with Table 2, we can see that the intra-day dynamic pattern “ss” accounts for the largest degree for all three crude oil futures. Table 3 documents the transition edges and shows that the pattern “ss” will most likely still be followed by “ss” on the next day. The second-largest degree node is slightly divergent between INE and benchmarks, resulting in the pattern “sr” for INE and the pattern “ds” for WTI and Brent, but both are often followed by the pattern “ss”. The degree of remaining nodes is mixing, and the weights of corresponding edges are not particularly dominated. Regarding the measure of betweenness, the pattern “rs” wins first place for INE, while the largest betweenness node for WTI and Brent is “ss”. This implies that different from the international benchmarks whose central intra-day movement patterns are likely to be the same during day and night trading sessions, INE is likely to be varied. The node with the second-largest betweenness is more divergent among all three futures, appearing the pattern “rd” for INE, and the patterns “sr” and “dr” for WTI and Brent, respectively. Lastly, to compare the measure of closeness, we find that the largest closeness node is the pattern “dd” for INE and Brent, and the pattern “sd” for WTI. Similar to the betweenness, the second-largest closeness node becomes more disparate, giving the pattern “dd” for INE, “sd” and “dd” for WTI and Brent, respectively. The mixing results on the exposed intra-day movement structures indicate that, although INE shows

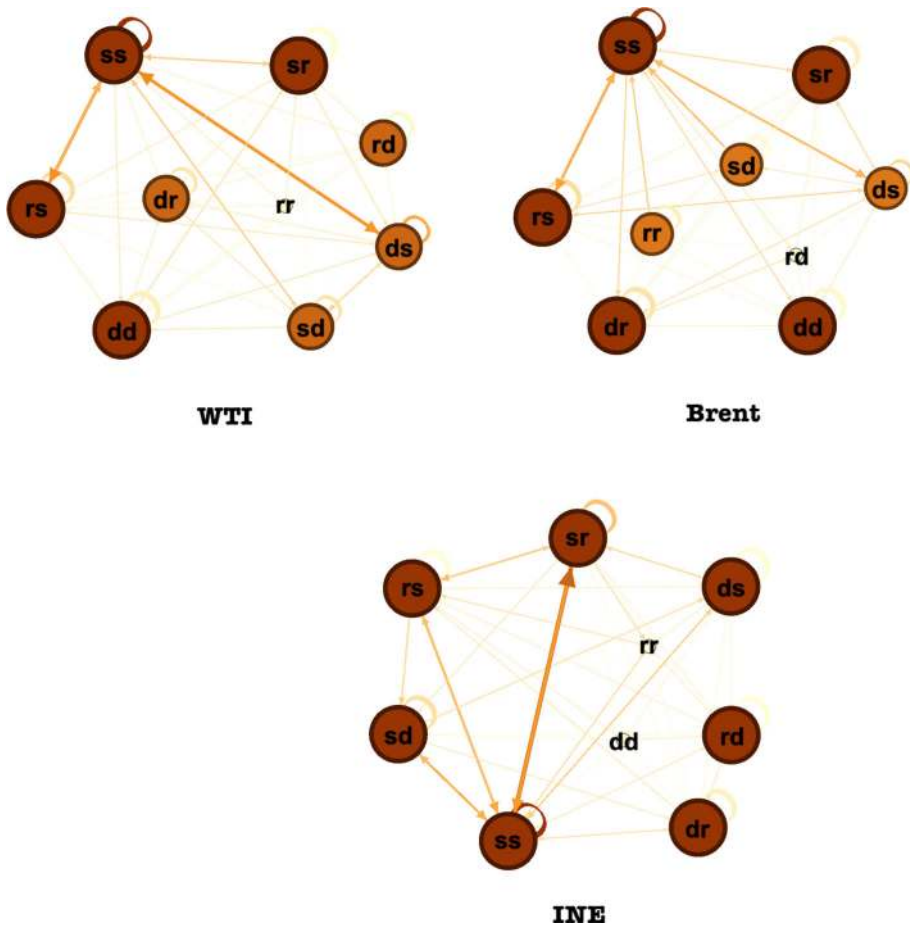


Fig. 4 Complex networks built on intra-day dynamic modes of INE, WTI and Brent crude oil

some integration with WTI and Brent, it still shows some regional market segmentations. This regional segmentation motivates us further to study the co-movements between INE and WTI and Brent.

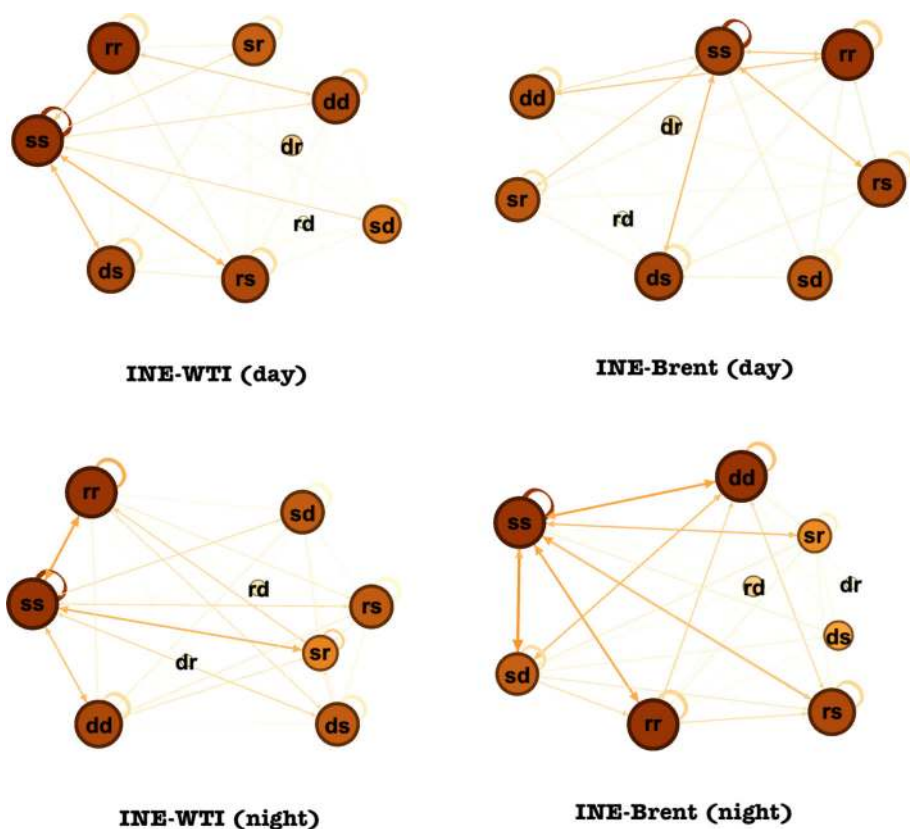
As discussed in Sect. 2.2, the network models with the nodes taking the form of {INE pattern, benchmark pattern} were constructed to analyse the dynamics of intra-day co-movements. In order to study their co-movements between day and night trading sessions, we build the networks separately toward these two trading sessions. Figure 5 shows virtual plots of the complex network between INE and the international benchmarks in the day and night trading sessions, respectively. In all networks, we find that the three largest degree nodes are the patterns “ss”, “rr” and “dd”, and it is also noticeable that the nodes of divergent patterns “rd” and “dr” are very rare with the smallest degrees. These results indicate a general trend of co-movements in the global crude oil futures market. Nonetheless, to compare the complex networks between day and night sessions, it is notable that the co-movement nodes are dominated during night sessions, while these nodes are less dominated in the day

Table 2 Degree, betweenness and closeness centralities of INE, WTI and Brent networks with all values measured in percentages

Rank	Degree	Betweenness						Closeness											
		INE		WTI		Brent		INE		WTI		Brent							
		Label	Value	Label	Value	Label	Value	Label	Value	Label	Value	Label	Value						
1		ss	27.31	ss	27.15	ss	29.00	rs	35.00	ss	42.52	ss	55.24	dd	11.25	sd	11.61	dd	11.39
2		sr	15.74	ds	16.78	ds	13.96	rd	20.00	sr	22.18	dr	12.42	rd	11.25	dr	11.61	ss	11.39
3		rs	12.27	rs	11.70	rs	12.77	ss	17.50	dd	15.01	rs	11.54	rs	11.25	ss	11.61	rs	11.39
4		sd	10.53	sr	9.49	dr	9.74	ds	15.00	rs	10.20	sr	9.23	sd	11.25	rd	11.61	rr	11.39
5		ds	8.80	sd	9.16	sr	8.44	dr	5.00	ds	5.67	dd	6.35	ds	11.25	rs	11.61	rd	11.39
6		rr	7.18	dd	8.50	dd	7.47	sr	5.00	sd	1.70	ds	2.60	dr	11.25	sr	11.61	sr	11.39
7		dr	7.18	dr	7.51	sd	7.14	sd	2.50	dr	1.70	sd	1.54	ss	11.25	dd	11.61	dr	11.39
8		rd	6.25	rd	5.52	rr	6.06	dd	0.00	rd	1.02	rr	0.65	sr	11.25	ds	10.32	ds	10.13
9		dd	4.75	rr	4.19	rd	5.41	rr	0.00	rr	0.00	rd	0.44	rr	10.00	rr	8.44	sd	10.13

Table 3 Weights of the top five edges of INE, WTI and Brent complex networks with all values measured in percentages

Rank	INE		WTI		Brent	
	Edges	Weight	Edges	Weights	Edges	Weights
1	ss → ss	8.56	ss → ss	9.27	ss → ss	10.17
2	ss → sr	6.48	ds → ss	5.30	ss → rs	4.76
3	sr → ss	4.40	ss → rs	5.08	rs → ss	4.11
4	rs → ss	3.70	ss → ds	4.86	ss → ds	3.90
5	sd → ss	3.47	ds → ds	3.97	ds → ss	3.46

**Fig. 5** Complex networks built on intra-day co-movement modes of pair-wise crude oil futures between INE and WTI/Brent. The sub-figures in the first row represent networks in day trading sessions, and the sub-figures in the second row represent networks in the night trading session

network models. Once again, these findings confirm that the co-movements between INE and the global crude oil futures market become weak during the day trading sessions.

Additionally, the directional edges connect the nodes and reveal the transformation from a pattern to another, and the weights of edges measure the frequency of these transformations. An immediate application from this is that we can calculate the transition probability and

predict co-movement patterns. Inspired by Liu et al. (2017), we utilise the networks and calculated the transition probabilities between all nodes over the sample period. Using the transition matrices shown in Table 4, we get the probabilities of the next day's co-movement patterns between INE and WTI or Brent. It should be noted that these probabilities are highly sample-driven as the sample length and market status can be crucial factors in determining the accuracy of transition probability. Given that INE is still a young market and lacks plenty of historical data, some biases can be present. However, based on the truth that oil prices have a long memory characteristic supported by previous literature, we believe the transit probability estimators will be stable if more observations are included. The current sample retains some similarities on the transition probabilities between INE and two international leaders, which yields a correlation coefficient of 0.72 between INE-WTI (day) and INE-Brent (day) and 0.76 between INE-WTI (night) and INE-Brent (night). The relatively steady co-movement dynamics implies that we can take advantage of some regular transformation channels to hedge the trading risks between INE and international benchmarks.

4 Pairs trading strategy of crude oil futures

Despite the fact that INE is a new player in the global crude oil futures market, it has drawn increasing attention in terms of exploring trading opportunities. This section designs a pairs trading strategy based on intra-day co-movement dynamics indicated by the complex network models.

4.1 The pairs trading strategy and its performance

The previous section computed the day-by-day transition probabilities of intra-day co-movement patterns, which allow us to predict the co-movement pattern between INE and the international benchmarks. Thus, we allocate long positions between INE and other crude oil futures under a unit budget constraint. The following demonstrates the trading strategy with an example composed of INE and WTI, and the case of INE and Brent is essentially the same.

Assuming that the intra-day co-movement pattern can be precisely predicted from a transit probability \mathbb{P} , we generate three trading signals: "Buy INE", "Buy WTI", and "Equal weights for INE and WTI". The signal "Equal weights for INE and WTI" would be considered if the predicted co-movement between INE and WTI were concordant, i.e., {"ss", "rr", "dd"}. On the contrary, the signal "Buy INE" or "Buy WTI" would be identified if we predicted a divergent co-movement between INE and WTI. The following chart shows how to determine the trading signals based on the forecasting of divergent co-movement patterns. We take the first row in the left-hand side panel as an example. When the predicted co-movement pattern was "rs", with the meaning that INE and WTI are respectively to show "Rise" and "Sidewalk" patterns on the day $(i + 1)$, we assign a trading signal "Buy INE" at the end of the day (i) simply because INE outperforms under the prediction.

$$\text{Buy INE} \begin{cases} \text{INE Rise, WTI Sidewalk (rs)} \\ \text{INE Rise, WTI Decrease (rd)} \\ \text{INE Sidewalk, WTI Decrease (sd)} \end{cases}, \quad \text{Buy WTI} \begin{cases} \text{INE Decrease, WTI Sidewalk (ds)} \\ \text{INE Decrease, WTI Rise (dr)} \\ \text{INE Sidewalk, WTI Rise (sr)} \end{cases}$$

In practice, it is infeasible to predict a certain intra-day co-movement pattern under the transit probability matrix \mathbb{P} . Instead, it yields different possible co-movement patterns, which

Table 4 Transition probabilities of intra-day co-movement modes in complex networks between INE and WTI/Brent with all values measured in percentages

INE-WTI (day)										INE-Brent (day)									
ss	rr	rs	ds	dd	sr	sd	rd	dr		ss	rr	rs	ds	dd	sr	sd	rd	dr	
ss	40.41	10.27	14.38	10.96	6.85	6.85	2.05	1.37	ss	41.30	11.59	13.77	11.59	6.52	8.70	5.80	0.72	0	
rr	27.59	12.07	10.34	5.17	22.41	8.62	3.45	3.45	rr	20.59	17.65	11.76	5.88	22.06	8.82	8.82	1.47	2.94	
rs	35.71	14.29	16.07	12.50	7.14	5.36	7.14	0	rs	33.96	15.09	11.32	11.32	7.55	7.55	11.32	0	1.89	
ds	42.55	6.38	14.89	19.15	4.26	4.26	2.13	4.26	ds	38	12	12	16	6	6	8	2	0	
dd	21.28	29.79	10.64	6.38	19.15	4.26	2.13	6.38	dd	24.44	35.56	8.89	8.89	17.78	2.22	2.22	0	0	
sr	25.81	16.13	6.45	16.13	9.68	16.13	6.45	0	sr	30.56	8.33	11.11	16.67	5.56	22.22	5.56	0	0	
sd	42.31	11.54	11.54	15.38	7.69	3.85	7.69	0	sd	24.14	13.79	17.24	20.69	6.90	3.45	6.90	0	6.90	
rd	10	20	20	0	20	30	0	0	rd	33.33	0	33.33	0	0	33.33	0	0	0	
dr	14.29	14.29	14.29	14.29	14.29	0	28.57	0	dr	0	50.00	0	16.67	16.67	0	0	0	16.67	
INE-WTI (night)										INE-Brent (night)									
ss	rr	rs	ds	dd	sr	sd	rd	dr		ss	rr	rs	ds	dd	sr	sd	rd	dr	
ss	36.09	15.79	7.52	7.52	12.03	13.53	6.02	0.75	ss	31.75	13.49	8.73	2.38	14.29	10.32	16.67	1.59	0.79	
rr	28.95	25	9.21	11.84	5.26	11.84	3.95	1.32	rr	28.81	15.25	15.25	5.08	16.95	5.08	8.47	3.39	1.69	
rs	23.53	14.71	5.88	14.71	17.65	17.65	2.94	2.94	rs	34.69	12.24	16.33	4.08	16.33	6.12	6.12	2.04	2.04	
ds	27.78	19.44	2.78	11.11	5.56	19.44	8.33	0	ds	6.25	12.50	6.25	0	6.25	18.75	18.75	0	6.25	
dd	28.57	12.24	12.24	4.08	16.33	12.24	10.20	2.04	dd	23.19	11.59	13.04	4.35	17.39	7.25	18.84	1.45	2.90	
sr	30	20	6.67	1.67	13.33	20	8.33	0	sr	37.14	14.29	11.43	0	11.43	8.57	17.14	0	0	
sd	32.14	10.71	10.71	7.14	17.86	7.14	7.14	0	sd	25	15	10	6.67	21.67	6.67	11.67	3.33	0	
rd	33.33	33.33	16.67	0	0	0	16.67	0	rd	12.50	25	12.50	0	12.50	12.50	25	0	0	
dr	33.33	16.67	0	33.33	16.67	0	0	0	dr	33.33	16.67	0	16.67	33.33	0	0	0	0	

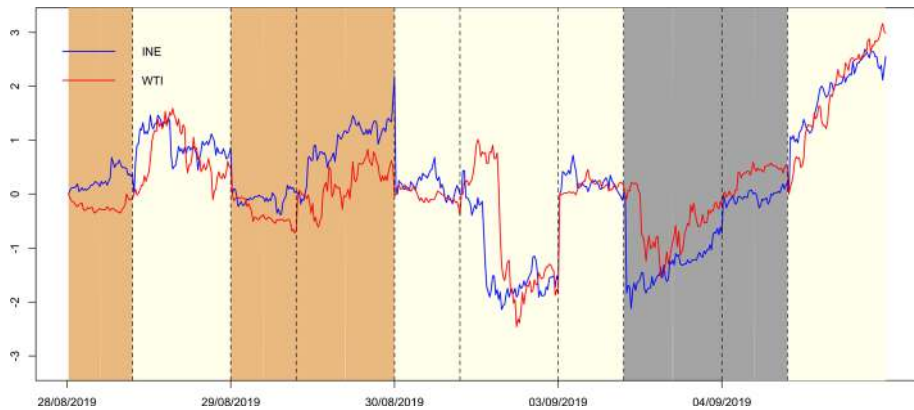


Fig. 6 Trading signals on INE and WTI crude oil futures, with orange, grey, and ivory shaded intervals standing for “Buy INE”, “Buy WTI” and “Equal weights”

suggests the weights allocated to three trading signals: $w_{i+1,EW}$, $w_{i+1,INE}$, and $w_{i+1,WTI}$, with the constraint $(w_{i+1,EW} + w_{i+1,INE} + w_{i+1,WTI}) = 1$. Consequently, the return of trading strategy y_{i+1}^{PT} can be computed as follows:

$$y_{i+1}^{PT} = (y_{i+1}^{INE}/2 + y_{i+1}^{WTI}/2) \times w_{i+1,EW} + y_{i+1}^{INE} \times w_{i+1,INE} + y_{i+1}^{WTI} \times w_{i+1,WTI}, \quad (2)$$

where y_{i+1}^{INE} and y_{i+1}^{WTI} are the realisation of closing returns on day $(i + 1)$. The transit probability matrix must be estimated from the historical data. Thus, we use $\hat{\mathbb{P}}$ as shown in Table 4. The pairs trading rule now can be summarised as:

Algorithm 1: Pairs trading strategy of crude oil futures

Input: Co-movement pattern on day (i) , $y_i^{INE}(t)$, $y_i^{WTI}(t)$, $\hat{\mathbb{P}}$.

Output: \hat{y}_{i+1}^{PT}

Step 1. Predict the intra-day co-movement pattern on day $(i + 1)$ by using a known transit probability matrix $\hat{\mathbb{P}}$;

Step 2. get the trading signals and assign weights to “Buy INE”, “Buy WTI”, and “Equal weights for INE and WTI”;

Step 3. obtain trading return y_{i+1}^{PT} according to Equation (2).

Figure 6 provides an example to illustrate how the trading strategy work over day and night trading sessions in five days. If an interval is shaded with “orange” or “grey”, we position “Buy INE” or “Buy WTI”; otherwise, we trade with “Equal weights”. The figure shows rational positioning weights on INE and WTI, given the fact that their co-movement patterns are precisely predicted. For example, on August 28, 2019, the position of “Buy INE” in the day session seems to be a wise decision given that the realisations of INE’s returns rise and WTI’s returns fall.

To evaluate the trading performance, we denote PT_{Isf} (intra-day co-movements forecasting) as the portfolio using the sample transition probability $\hat{\mathbb{P}}$. In addition, we consider a frictionless case that the intra-day co-movement patterns are precisely predicted without any bias from the sample, i.e., in-sample simulation, denoted by PT_{Ora} (oracle). Three benchmark assets are used, including INE, WTI or Brent, and an equal-weight portfolio (Ewgt).

Table 5 reports the annual return, Sharp ratio, and a maximum drawdown of the assets returns. A three-month T-bill rate is deployed as the risk-free rate in the Sharp ratio calculation. In specific, the portfolio PT_{Isf} always outperforms the benchmarks over both day and night trading sessions, producing higher Sharp ratios and much lower maximum drawdown during the day trading session. Even though its performance becomes weaker when we pairs trade INE and Brent, the findings remain robust. Second, the portfolio PT_{Ora} gains much higher Sharp ratios in all scenarios, which implies a potentially high profit if a more precise transition probability is used. Third, compared with day trading session, except for PT_{Ora} , all other portfolios perform clumsily during the night trading sessions. This is not too surprising as the hedging opportunities are lacking given more integrated night trading sessions, and also, the high violation in the night session leads to a difficult forecasting task. Nonetheless, PT_{Isf} still hedges some risks compared with benchmarks. Figure 7 plots the cumulative returns in the case of trading INE and WTI in day sessions. The coloured signals are used as the same as in Fig. 6. Consistently, the portfolio PT_{Isf} generally outperform the benchmarks, and the cumulative returns of PT_{Ora} rockets during the sample period benefit from the assumption that accurate transition probabilities are applied.

Furthermore, to explore the underlying regularities, we compute the Sharpe ratio of portfolio returns classified by intra-day co-movement patterns. Table 6 displays the Sharpe ratios of PT_{Isf} and PT_{Ora} ' returns categorised with nine types of co-movement patterns. According to the results, the portfolio PT_{Isf} is more likely to be profitable in the day trading sessions if the co-movement patterns were "ss", "rs", "dd", "sd", and "rd". In contrast, only the pattern "ds" consistently delivers positive profit in night trading sessions. In addition, the portfolio PT_{Ora} obtains positive profits under most intra-day co-movement patterns with only a few exceptions, including "rs", "dd", "sd" and "dr" in the night trading sessions. These findings confirm that the intra-day co-movements between INE and WTI or Brent have founded some repeatable regularities, which can be used to understand the dynamic co-movements and guide investments in the future global crude oil futures market.

4.2 Pairs trade crude oil futures during the COVID-19 pandemic

Lastly, we apply the pairs trading strategy during the period of the COVID-19 pandemic. The pandemic phase deserves a differential treatment considering the sharp slumps of global crude oil prices, and splitting sub-samples can account for potential structural breaks. For the pandemic effect on commodity and equity markets, we refer to Ji et al. (2020) and Zhang et al. (2020). Moreover, the INE's regulators suspended the night trading session during the first outbreak of the pandemic in order to avoid a catastrophic spillover effect from the global crude oil market. Despite the regulation, Yang et al. (2020) indicated a sharp increase in the risk spillover between Chinese and international crude oil futures, and similar findings are also evidenced by Lu et al. (2020). Under a context of high-risk fluctuations and strict market regulation, below we evaluate the robustness of pairs trading strategy based on the intra-day co-movement patterns over day trading sessions from January 2 to April 30, 2020.

Using the same methodology, we cluster the CIDR curves from the pandemic sub-sample into three categories: "s", "r" and "d", which are used to construct {INE pattern, benchmark pattern}-type nodes for building complex networks. Correspondingly, we obtain the COVID-19 sample-driven transit probability matrix in Table 4, advising the portfolio weights in the pairs trading strategy. Table 7 reports the annual return, Sharpe ratio, and a maximum drawdown of the portfolios. Overall, the performances are consistent. The portfolio PT_{Isf} does not experience a dramatic loss compared with the benchmarks, albeit it is less profitable than

Table 5 Performance of the returns of INE and WTI/Brent crude oil futures and corresponding pairs trading strategies

Panel A: INE and WTI									
	Day			Night					
	INE	WTI	Ewgt	PT _{Isf}	PT _{Ora}	INE	WTI	Ewgt	PT _{Ora}
Annual return	9.52	3.81	6.67	7.92	36.61	− 20.14	− 19.92	− 20.03	− 17.47
Sharpe ratio	0.0417	0.0139	0.0338	0.0434	0.2419	− 0.0564	− 0.0595	− 0.0619	− 0.0551
Max drawdown	12.00	7.29	8.77	9.01	7.14	58.34	51.33	52.92	50.43
Panel B: INE and Brent									
	INE	WTI	Ewgt	PT _{Isf}	PT _{Ora}	INE	WTI	Ewgt	PT _{Ora}
Annual return	9.52	2.10	5.81	7.43	32.70	− 20.14	− 26.14	− 23.14	− 22.53
Sharpe ratio	0.0417	0.0006	0.0267	0.0391	0.2180	− 0.0564	− 0.0849	− 0.0741	− 0.0718
Max drawdown	12.00	9.51	8.93	8.66	11.03	58.34	59.97	57.47	57.68

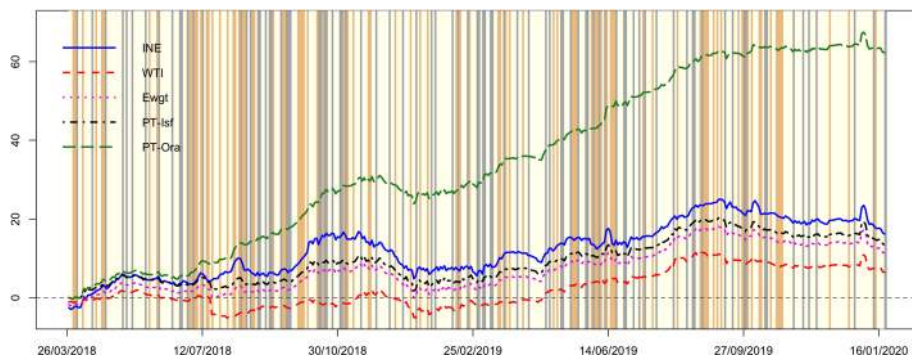


Fig. 7 The cumulative returns of INE and WTI crude oil futures and their pairs trading strategies in day trading sessions

the market normal phase. We attribute this to the sample estimator bias of transit probabilities. With precise transit probabilities, the portfolio PT_{Ora} gains promising performance with a high Sharpe ratio and low maximum drawdown. Figure 8 displays the portfolios' cumulative returns related to INE and WTI, and they generally show consistent performance. Besides, we observe that the trading signals are increasingly changeable during market turmoil, reflecting that the co-movement patterns between INE and the international benchmarks are more variant during the crisis. This is a result mainly due to the segmented local regulations, further enhancing the regional market fractional effect. Similar patterns are also shown in Fig. 7 given elusive trading signals during the second half of 2018, which can be driven by a series of events affecting the oil price, such as the Iranian sanctions. Following the market normal sample analysis, we also calculate the Sharpe ratios of the portfolio returns classified by intra-day co-movement patterns. Table 8 shows that the pairs trading strategies are more likely to be profitable when the co-movement modes are “ss”, “rr”, “rs”, “dd” and “sd”. This result is consistent with the previous findings and indicates a robust performance of the pairs trading strategy during the market crash.

Identifying some market fractional effect during the market turmoil period is, to some extent, unexpected but interesting. The typical thought would be an increasing integration under such a severe global shock, which may occur due to the rapid spread of investor panic. A closer look at the pandemic may reveal the reasons for this finding. First, the outbreak of COVID-19 has a clear chronological order. While the epidemic started the first in China, it was suppressed quickly by the efforts of the Chinese government. Unfortunately, the large-scale spreads carry on hitting Europe and the U.S., creating clear differences across markets. Second, the cross-market segmentation may also due to differences in market trading mechanisms. In the INE market, investors have a strong expectation for a bottom price of oil and thus willing to hold long positions when prices are low, whereas the same support does not exist for the international benchmarks. Pessimistic investors can drive the price to a much lower level.

Table 6 Sharpe ratio of returns of pairs trading strategies in different types of intra-day co-movement modes

	ss	rr	rs	ds	dd	sr	sd	rd	dr
PT _{I_{sf}}	INE-WTI(day)	0.0563	-0.1376	0.2096	-0.0437	0.0467	0.1894	0.4948	-0.1176
	INE-WTI(night)	-0.0820	0.0481	-0.1543	0.0755	-0.1578	-0.1541	0.1791	-0.2352
	INE-Brent(day)	0.1121	-0.0054	0.1037	-0.1078	0.0623	0.0238	1.9093	0.1095
	INE-Brent(night)	-0.0208	-0.1371	0.0149	0.2156	-0.1204	-0.1358	-0.0283	-0.3140
	INE-WTI(day)	0.2941	-0.0023	0.4124	0.2781	0.1362	0.3464	0.7427	0.1121
PT _{Ora}	INE-WTI(night)	0.0105	0.2469	-0.0380	0.2581	-0.0937	0.1358	0.2864	-0.2192
	INE-Brent(day)	0.2584	0.1358	0.3106	0.1512	0.1077	0.3278	1.3684	0.2821
	INE-Brent(night)	0.0716	0.0240	0.1314	0.4798	0.0003	-0.0247	0.0741	-0.2984

Table 7 Performance of returns of INE and WTI/Brent crude oil futures and corresponding pairs trading strategies during the COVID-19 pandemic

	INE and WTI			INE and Brent						
	INE	WTI	Ewgt	PT _{ISF}	PT _{Ora}	INE	Brent	Ewgt	PT _{ISF}	PT _{Ora}
Annual return	-28.97	-33.71	-31.34	-2.88	176.40	-28.97	-32.96	-30.97	-39.31	89.76
Sharpe ratio	-0.0498	-0.0285	-0.0483	-0.0072	0.1899	-0.0498	-0.0358	-0.0514	-0.0587	0.1655
Max drawdown	18.28	44.08	22.49	18.04	10.62	18.28	38.87	27.89	30.45	6.90

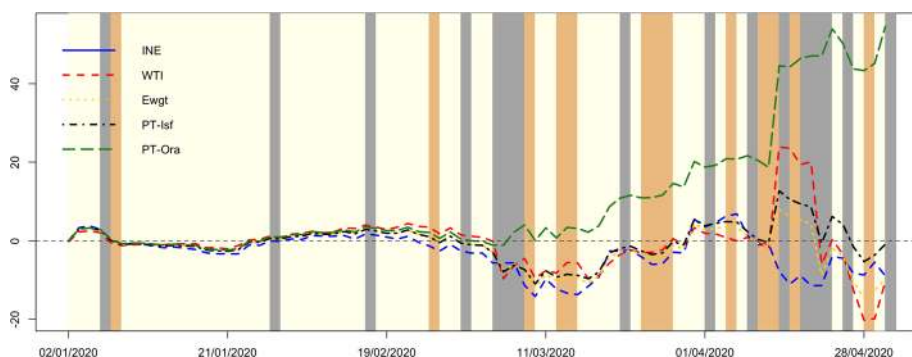


Fig. 8 The cumulative returns of INE and WTI crude oil futures and their pairs trading strategies during the COVID-19 pandemic

5 Conclusion

In this paper, we focused on the dynamic intra-day co-movements between China's INE crude oil futures and the international benchmark WTI and Brent crude oil futures. Based on a five-minute frequency dataset from March 2018 to April 2020, a functional data clustering approach was applied to categorize intra-day return curves into three intra-day movement groups—"Rise", "Decrease", and "Sidewalk". We then constructed complex network models to investigate the interrelationships and co-movements of the intra-day movement patterns for both a single market and three markets as a system. The main finding is two-fold. First, INE behaves disparately in its co-movements with WTI and Brent over the day (9:00 a.m.–11:30 a.m. and 1:30 p.m.–3:00 p.m.) and night (9:00 p.m.–2:30 a.m.) trading sessions. In particular, the co-movements between INE and the international benchmarks are weak during the day trading session, displaying the feature of the regional fractional market, while INE becomes more like a follower to WTI and Brent during the night trading sessions. Second, under the local market regulations, INE's regional market fractional effect is enhanced during the market turmoil period, making this market less integrated with the global crude oil futures market. Besides, as an application of the main results, we simulated a pairs trading strategy of INE and international benchmarks to explore hedging opportunities for investors. We showed that benefit from a regional fractional effect, our trading strategy is profitable during day trading sessions even under a market turmoil phase suffered from the recent COVID-19 pandemic. It is also profitable during night trading sessions if the intra-day co-movement patterns are more precisely predicted.

Our findings provide implications to policymakers to understand the impact of current regulations and make the response to global crude oil market shocks. With the increasing marketization and maturity of China's crude oil futures, its price behaviour will be gradually synchronized with the international price. The drastic price fluctuation and risk transmission in the international crude oil market will inevitably increase the investment risk and market instability of the domestic crude oil futures market. Investors need to adopt a more cautious and prudent investment attitude, pay more attention to the information dynamics of the international market, and establish the INE-benchmark linked risk monitoring model to deal with the impact of international input risk. The regulators in China should continue to improve and optimize the crude oil futures trading mechanism, deeply understand market participants'

Table 8 Sharpe ratio of returns of pairs trading strategies in different types of intra-day co-movement modes during the COVID-19 pandemic

		ss	rr	rs	ds	dd	sr	sd	rd	dr
PT_{Isf}	INE-WTI	0.1273	0.0484	0.0100	-0.4729	0.1108	0.5957	1.1625	0.2514	-0.7859
	INE-Brent	0.1244	0.2603	-0.1286	-0.5549	0.6682	-1.2572	1.3409	-0.3328	-0.5855
PT_{Ora}	INE-WTI	0.2732	0.1644	0.3272	-0.0387	0.7920	0.8116	2.0569	1.4922	-0.5644
	INE-Brent	0.2246	0.2713	0.2761	-0.0804	0.8652	0.0566	2.5623	-0.3328	-0.5085

needs, establish an industry database and information release mechanism, and provide a trading reference for domestic and international crude oil futures participants. By constantly improving the market system and trading mechanism, market access and risk supervision system, and cooperating with RMB's internationalization strategy, the international influence of China's crude oil futures will be improved. Additionally, due to the differences in the design of crude oil futures contract systems at home and abroad, there may be a mismatch of the inner and outer layers to a certain extent. Therefore, China should promote its crude oil futures' trading effectiveness in the future, taking into account the controllable risk and market liquidity.

Future work should concentrate on analyse further the characteristics of dynamic volatility spillover effect between domestic and foreign crude oil futures markets, explore the dynamic risk contagion mechanism, and try to carry out the research on dynamic portfolio hedging. Also, calibrating the estimator of transit probability matrix for intra-day co-movement patterns can be crucial when more INE observations become available, and studying the co-movements between WTI, Brent, and INE under the effect of U.S. energy independence is also of interest.

Acknowledgements The authors would like to thank the editor and three anonymous referees. Their detailed and insightful comments and suggestions have improved the content of this paper. Of course, all errors remain our own.

Author Contributions QJ: Conceptualization, methodology, writing-original draft preparation, reviewing and editing, validation. DZ: Conceptualization, supervision, reviewing and editing, validation. YZ: Methodology, software, writing-original draft preparation, investigation.

Funding This research is supported by the National Social Science Foundation of China (NSSFC) Major project Grant No. 20&ZD110.

Data availability The paper uses WTI and Brent crude oil futures data obtained from Eikon-Thomson and Reuters and INE crude oil futures data from WIND Financial Databases. The three-month Treasury-bill rate is downloaded from Yahoo Finance. All data used in this paper is available upon request. **Code availability** R code for data cleaning and analysis is available upon request.

Declarations

Conflict of interest No potential competing interest was reported by the authors.

References

- AlMadi, M. S., & Zhang, B. (2011). Lead-lag relationships between world crude oil benchmarks: Evidence from West Texas Intermediate, Brent, Dubai and Oman. *International Research Journal of Finance and Economics*, 80, 13–26.
- Birgé, L., & Massart, P. (2007). Minimal penalties for Gaussian model selection. *Probability Theory and Related Fields*, 138(1–2), 33–73.
- Bouveyron, C., Côme, E., & Jacques, J. (2015). The discriminative functional mixture model for a comparative analysis of bike sharing systems. *The Annals of Applied Statistics*, 9(4), 1726–1760.
- Bouveyron, C., & Jacques, J. (2011). Model-based clustering of time series in group-specific functional subspaces. *Advances in Data Analysis and Classification*, 5(4), 281–300.
- Caporin, M., Fontini, F., & Talebbeydokhti, E. (2019). Testing persistence of WTI and Brent long-run relationship after the shale oil supply shock. *Energy Economics*, 79, 21–31.

- Chen, W., Huang, Z., & Yi, Y. (2015). Is there a structural change in the persistence of WTI-Brent oil price spreads in the post-2010 period? *Economic Modelling*, 50, 64–71.
- Gai, P., & Kapadia, S. (2010). Contagion in financial networks. *Proceedings of the Royal Society A: Mathematical, Physical and Engineering Sciences*, 466(2120), 2401–2423.
- Górecki, T., Hörmann, S., Horváth, L., & Kokoszka, P. (2018). Testing normality of functional time series. *Journal of Time Series Analysis*, 39(4), 471–487.
- Hammoudeh, S. M., Ewing, B. T., & Thompson, M. A. (2008). Threshold cointegration analysis of crude oil benchmarks. *The Energy Journal*, 29(4).
- Horváth, L., Kokoszka, P., & Rice, G. (2014). Testing stationarity of functional time series. *Journal of Econometrics*, 179(1), 66–82.
- Huang, X., & Huang, S. (2020). Identifying the comovement of price between China's and international crude oil futures: A time-frequency perspective. *International Review of Financial Analysis*, 72, 101562.
- Ji, Q., & Fan, Y. (2015). Dynamic integration of world oil prices: A reinvestigation of globalisation vs. regionalization. *Applied Energy*, 155, 171–180.
- Ji, Q., & Zhang, D. (2019). China's crude oil futures: Introduction and some stylized facts. *Finance Research Letters*, 28, 376–380.
- Ji, Q., Zhang, D., & Zhao, Y. (2020). Searching for safe-haven assets during the COVID-19 pandemic. *International Review of Financial Analysis*, 71, 101526.
- Jia, X., An, H., Fang, W., Sun, X., & Huang, X. (2015). How do correlations of crude oil prices co-move? A grey correlation-based wavelet perspective. *Energy Economics*, 49, 588–598.
- Kearney, F., & Shang, H. L. (2020). Uncovering predictability in the evolution of the WTI oil futures curve. *European Financial Management*, 26(1), 238–257.
- Klein, T. (2018). Trends and contagion in WTI and Brent crude oil spot and futures markets: The role of OPEC in the last decade. *Energy Economics*, 75, 636–646.
- Kokoszka, P., Rice, R., & Shang, H. L. (2017). Inference for the autocovariance of a functional time series under conditional heteroscedasticity. *Journal of Multivariate Analysis*, 162, 32–50.
- Li, H., & Lin, S. X. (2011). Do emerging markets matter in the world oil pricing system? Evidence of imported crude by China and India. *Energy Policy*, 39(8), 4624–4630.
- Li, P., Huang, L., & Li, P. (2020). Are Chinese crude oil futures good hedging tools? *Finance Research Letters*, 101514.
- Li, R., & Leung, G. C. K. (2011). The integration of China into the world crude oil market since 1998. *Energy Policy*, 39(9), 5159–5166.
- Liu, B. Y., Ji, Q., & Fan, Y. (2017). A new time-varying optimal copula model identifying the dependence across markets. *Quantitative Finance*, 17(3), 437–453.
- Lu, X., Ma, F., Wang, J., & Wang, J. (2020). Examining the predictive information of CBOE OVX on China's oil futures volatility: Evidence from MS-MIDAS models. *Energy*, 212, 118743.
- Narayan, P. K., Narayan, S., & Popp, S. (2011). Investigating price clustering in the oil futures market. *Applied Energy*, 88, 397–402.
- Palao, F., Pardo, Á., & Roig, M. (2020). Is the leadership of the Brent-WTI threatened by China's new crude oil futures market? *Journal of Asian Economics*, 101237.
- Ramsay, J. O., & Silverman, B. W. (2007). *Applied functional data analysis: Methods and case studies*. Berlin: Springer.
- Rice, G., Wirjanto, T., & Zhao, Y. (2020a). Forecasting value at risk with intra-day return curves. *International Journal of Forecasting*, 36(3), 1023–1038.
- Rice, G., Wirjanto, T., & Zhao, Y. (2020b). Tests for conditional heteroscedasticity of functional data. *Journal of Time Series Analysis*, 41(6), 733–768.
- Sugar, C. A., & James, G. M. (2003). Finding the number of clusters in a dataset: An information-theoretic approach. *Journal of the American Statistical Association*, 98(463), 750–763.
- Wang, M., Chen, Y., Tian, L., Jiang, S., Tian, Z., & Du, R. (2016). Fluctuation behavior analysis of international crude oil and gasoline price based on complex network perspective. *Applied Energy*, 175, 109–127.
- Wang, F., Ye, X., & Wu, C. (2019). Multifractal characteristics analysis of crude oil futures prices fluctuation in China. *Physica A: Statistical Mechanics and its Applications*, 533, 122021.
- Yang, C., Lv, F., Fang, L., & Shang, X. (2019). The pricing efficiency of crude oil futures in the Shanghai International Exchange. *Finance Research Letters*, 101329.
- Yang, Y., Ma, Y. R., Hu, M., Zhang, D., & Ji, Q. (2020). Extreme risk spillover between Chinese and global crude oil futures. *Finance Research Letters*, 101743.
- Zhang, B. (2019). Are Chinese and international oil markets integrated? *International Review of Economics & Finance*, 62, 41–52.
- Zhang, D., Hu, M., & Ji, Q. (2020). Financial markets under the global pandemic of COVID-19. *Finance Research Letters*, 36, 101528.

Zhu, Y., Yang, F., & Ye, W. (2018). Financial contagion behavior analysis based on complex network approach. *Annals of Operations Research*, 268(1–2), 93–111.

Publisher's Note Springer Nature remains neutral with regard to jurisdictional claims in published maps and institutional affiliations.